Resonant and thermal changes of refractive index in a heavily doped erbium fiber pumped at wavelength 980 nm

Yu. O. Barmenkov[a] and A. V. Kir'yanov[a]
Centro de Investigaciones en Optica, Loma del Bosque 115, Leon, Guanajuato, 37150 Mexico

M. V. Andrés
Departamento de Física Aplicada, Universidad de Valencia, Dr. Moliner 50, E46100 Burjassot, Spain

We report a theoretical and experimental study of the refractive index variation in a heavily doped erbium silica fiber within the spectral range 1500–1580 nm under the pumping at the wavelength 980 nm. The two main contributions in the refractive index change are addressed—the resonant part determined by the saturation effect in the fiber and the thermal part stemming from the fiber heating due to the excited-state absorption and Stokes losses. We demonstrate that the thermal contribution in the resultant refractive index change is a notable value, which is the feature of erbium fibers with a high concentration of erbium ions. © *2004 American Institute of Physics.*
[DOI: 10.1063/1.1787151]

The nonlinear optical properties of rare-earth-doped silica fibers have been under extensive investigation during the last decade. An importance of understanding of the nonlinear refraction features in such fibers, and particularly in the erbium ones, is caused by the needs of the fiber-optics communication and switching, engineering with erbium fiber amplifiers and lasers, etc. To date, various mechanisms have been investigated of the nonlinear change of refractive index in erbium silica fibers. The most studied is the change connected with the material dispersion of erbium fibers that is strictly, by the Kramers–Kronig relations (KKR), related to the change of erbium absorption spectrum under the optical pumping.[1–4] Another mechanism of the refractive index change is caused by the thermal dispersion and thermally induced stresses,[5,6] stemming from an inhomogeneous heating of the optically pumped fibers. The latter is mainly an appearance of the Stokes loss, given by the ratio of the pump and emission (lasing) wavelengths, and the excited-state absorption (ESA) loss, inevitably present in erbium fibers.[7–10]

In this letter, we report an experimental and theoretical investigation of the refractive index change in heavily doped erbium silica fiber within the spectral range 1500–1580 nm under the pumping at the wavelength $\lambda_{\text{pump}}=980$ nm, paying special attention to an accurate account of both the resonant and thermal contributions in the refractive index change.

An experimental study of the nonlinear refractive index change in an erbium-doped fiber was performed by the use of an electrically on/off-switched (rectangular signal, 20 Hz) pump diode laser, a Michelson fiber interferometer (MFI) with a tunable (wavelength range, 1500–1580 nm) low-power coherent semiconductor laser as a source of a probe signal, and a piezoceramics-based fiber modulator providing a phase modulation (PM) between the two optical waves in the interferometer's arms (Fig. 1). The two MFI arms were the cleaved fiber pieces, both having the reflection coefficients of about 4% on their free edges, with one of the pieces being a standard communication fiber and another—a 7.5-cm single-mode silica fiber (SLC 110-01, IPHT, Jena, Germany) with a high (2300 mol ppm) concentration of erbium

ions and the cutoff wavelength 1040 nm. A high-frequency (~50 kHz) PM signal with the modulation amplitude of about π radians was biased to the passive communication fiber, while the active (erbium) fiber was pumped by the pigtailed diode laser.

The setup arrangement allowed us to measure a phase shift between the optical waves, twice (forward-and-backward) propagating through the MFI arms. This shift occurs at the switching pump power on/off due to the change of a core refractive index, resulting in the change of an optical path in the MFI's active arm. The phase shift moves the interferometer's work point, which, in turn, changes the initial phase of the PM signal, affecting the shape of the modulation signal recorded by a photodetector. A simple analysis of the resultant signal allowed us to measure the refractive index change in the active erbium fiber.

The experimentally measured steady-state pump-induced wavelength-dependent phase shift $\Delta\varphi_{\text{res}}$ and the correspondent refractive index change Δn_{res} in the active fiber, obtained for several powers of the probe signal and a 70 mW pump power, are shown in Fig. 2 (pointed curves). The change Δn_{res} (Fig. 2, right axis) was calculated as

$$\Delta n_{\text{res}}(\lambda) = \frac{\Delta\varphi_{\text{res}}(\lambda)}{2\pi}\frac{\lambda}{2L}\frac{1}{\Gamma_1}, \tag{1}$$

where λ is the wavelength of the tunable laser, $L=7.5$ cm is the active fiber length, and $\Gamma_1=0.44$ is the core-beam overlap factor for the erbium fiber at $\lambda\approx1550$ nm. The maximum and minimum variations in the fiber core refractive index (4.5×10^{-6} and -1.2×10^{-6}) are observed, respectively, at the signal wavelengths $\lambda=1520$ and 1570 nm, whereas there is no noticeable change in the index (at least, at the steady state) within the interval $\lambda=1535–1550$ nm.
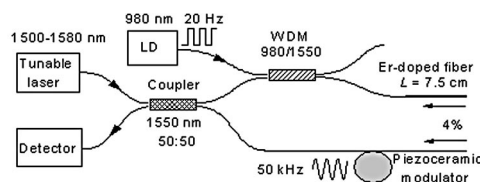

FIG. 1. The MFI–Michelson fiber interferometer.

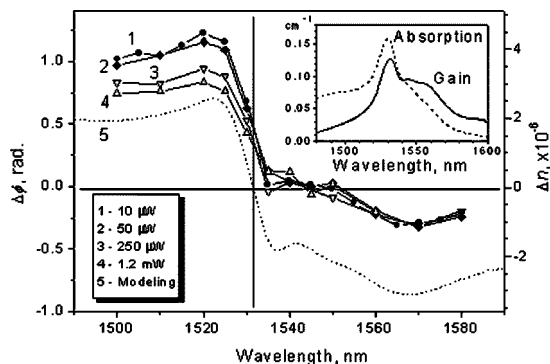[a]Author to whom correspondence should be addressed; electronic mail: yuri@cio.mx and kiryanov@cio.mx

FIG. 2. Experimental dependencies of phase shift (left) and refractive index change (right) versus wavelength of the signal wave. Curves 1–4 are measured for different signal-wave powers (see inset at the left) and pump power $P=70$ mW; curve 5 is the correspondent theoretical dependence built with the use of the KKR and the experimental data on absorption and gain spectra of the fiber presented in inset on the right.
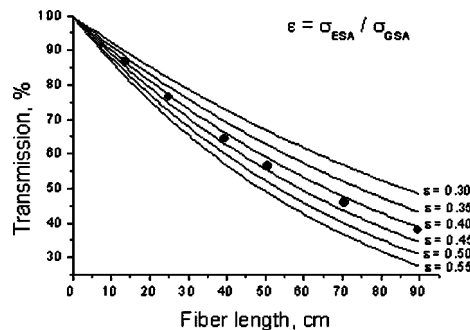

FIG. 3. Experimental (dots) and theoretical (lines) dependencies of the erbium fiber transmission vs its length (pump power—$P=50$ mW). A set of theoretical curves is built for the different ($\varepsilon=0.3-0.55$) values of ESA loss in the fiber and $P=50$ mW.

Note that at the signal powers exceeding $\sim100-150$ μW, the resonant refractive index change is saturated in-line with the resonant absorption saturation—compare the curves $3(250$ μW$)$ and $4(1.2$ mW$)$ with the curves 1 and 2 registered at the extremely low-power probing (10 and 50 μW, respectively). Meanwhile, an independent analysis of the power-dependent transmittance of the erbium fiber has shown that, e.g., the saturating power at $\lambda=1530$ nm is $P_{s,1530}\approx150$ μW.

However, the main deduction from Fig. 2 is that a character of the resonant refractive index change in the active fiber is different from the experimental data, relating the case of the fibers with low erbium doping,[5,11] as from the classical theoretical predictions, based on the modeling of Δn_{res}, using the KKR.[1,12] The latter is seen from a comparison of the experimental curves 1–4 with the theoretical curve 5 (see Fig. 2) for $\Delta n_{res}=\Delta\chi'/2n$ that has been calculated with the use of the experimental data for the ground-state absorption (GSA) and gain coefficients of the erbium fiber (see the right inset in Fig. 2) and the formula for the real part of atomic susceptibility[12] χ':

$$\chi'(\omega) = -\frac{nc}{\pi\omega}P.V.\int_{-\infty}^{+\infty}\frac{\sigma_{gain}(\omega')N_2-\sigma_{gsa}(\omega')N_1}{\omega'-\omega}d\omega', \quad (2)$$

which leads to the following formula for the resonant refractive index change:

$$\Delta n_{res} = \frac{\Delta\chi'(\omega)}{2n} = \frac{\chi'(\omega,t=\infty)-\chi'(\omega,t=t_0)}{2n}$$

$$\approx -\frac{c}{2\pi\omega}P.V.\int_{-\infty}^{+\infty}\frac{\alpha_0(\omega')+g_0(\omega')}{\omega'-\omega}d\omega'. \quad (3)$$

In formulas (2) and (3), n is the undisturbed fiber core refractive index, c is the velocity of light, ω is the angular frequency of the probe wave, σ_{gain} and σ_{GSA} are the gain and GSA cross sections, N_1 and N_2 are the population densities of erbium ions in the ground and excited states, respectively, $\alpha_0(\omega)=\sigma_{GSA}(\omega)N_0$ is the erbium fiber nonsaturated absorption coefficient, and $g_0(\omega)=\sigma_{gain}(\omega)N_0$ is the full-saturated gain coefficient. Note that formula (3) above is obtained for the case of a low-power signal wave, where, before the pump switching on, the number of erbium ions in the excited state can be ignored [$N_1(t<t_0)=N_0$ and $N_2(t<t_0)=0$; t_0 is the mo-

ment of the pump switching], and, after switching the pump ($P=70$ mW) on, practically all ions are in the excited state ($P_{s,980}\approx1.1$ mW), i.e., $N_1(t\rightarrow\infty)\approx0$ and $N_2(t\rightarrow\infty)\approx N_0$.

We have supposed that the nonexpected behavior of the refractive index change (Fig. 2) can be connected with an additional contribution in its resultant value stemming from the thermal effect in the erbium heavily-doped fiber. Therefore, the specific losses mentioned above (the ESA and Stokes losses) may play a considerable role in an extra (nonresonant) change of the refractive index.

To address the last effect, we have performed a set of experiments for clarifying an appearance of the ESA and Stokes losses in the fiber under study. Figure 3 shows the experimental dependencies (dots) of the fiber nonlinear transmission versus its length. In the same plot, are shown the correspondent theoretical dependencies calculated with the use of the equation addressing the saturation effect in an erbium fiber in the presence of ESA at the pump wavelength:

$$\frac{dI_p}{dz} = -\alpha_0 I_p\left[1-(1-\varepsilon)\frac{I_p}{I_p+I_{sat}}\right], \quad (4)$$

where $I_p=P/S_p$ is the intensity of the pump wave propagating through the fiber (S_p is the geometrical cross-section of the multimode pump-wave in the fiber), I_{sat} is the pump saturating intensity, α_0 is the low-signal pump absorption coefficient at $\lambda=\lambda_{pump}$, and $\varepsilon=\sigma_{ESA}/\sigma_{GSA}$ is the ratio of the GSA (σ_{GSA}) and ESA (σ_{ESA}) cross-sections in the erbium fiber.

As it is seen from the graphs, the best fitting of the experimental data by the theory is observed for the ratio $\varepsilon=0.43$. Note that the found value for the ESA-assisted loss $\lambda=\lambda_{pump}$ allows one to estimate the correspondent ESA cross-section in erbium fiber: $\sigma_{ESA}\approx0.5\times10^{-21}$ cm^2.

In order to calculate the wanted thermal contribution in the refractive index change in the erbium fiber, one should numerically calculate the temperature distribution across the fiber cross section, which is an indication of the pump-induced fiber heating, determined by the ESA loss ε and the Stokes loss, $\xi=1-\lambda_{pump}/\lambda$ and addressed in terms of the volumetric heat density Q:

$$Q = \alpha_0 I_p\left[\frac{I_p}{I_p+I_{sat}}(\varepsilon-\xi)+\xi\right]. \quad (5)$$

The latter formula allows one to easily find the resultant refractive index change Δn_{therm} (and the thermoinduced phase shift $\Delta\varphi_{therm}$) in the erbium fiber:
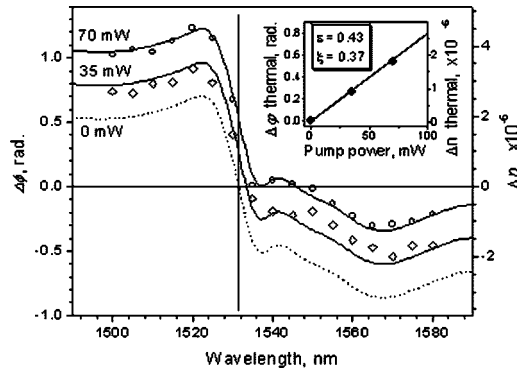
FIG. 4. Experimental (dots) and theoretical (lines) dependencies of overall phase-shift (left) and refractive index change (right) versus signal-beam wavelength for the different ($P=35$ and 70 mW) pump powers. Inset—dependencies of the thermal-induced contributions in phase-shift and refractive index vs pump power ($\lambda_{\text{pump}}=980$ nm).

$$\Delta n_{\text{therm}} = \frac{\lambda}{2\pi L}\Delta\varphi_{\text{therm}} = 2\frac{dS}{dT}\Delta T(Q,r), \qquad (6)$$

with the coefficient[6,13,14] dS/dT, being the total thermoinduced optical path change at the probe wavelength λ under the pumping by continuous wave radiation at the wavelength λ_{pump}, and the difference $\Delta T(Q,r)$ [between the temperatures inside the fiber, $T(Q,r)$, and on its outer surface, T_0], being:

$$\Delta T(Q,r) \equiv T(Q,r) - T_0$$
$$= \begin{bmatrix} \dfrac{qr_0^2}{2}\left[\dfrac{1-\left(\dfrac{r}{r_0}\right)^2}{2\Lambda_t} + \dfrac{\ln\left(\dfrac{R}{r_0}\right)}{\Lambda_t} + \dfrac{1}{Rh} \right], & r \leq r_0 \\[4mm] \dfrac{Qr_0^2}{2}\left[\dfrac{\ln\left(\dfrac{R}{r}\right)}{\Lambda_t} + \dfrac{1}{Rh} \right], & r > r_0, \end{bmatrix}$$
$$(7)$$

where r is the current radial coordinate across the fiber, $r_0 = 1.42$ μm is the radius of its erbium-doped area, $R = 62.5$ μm is the fiber outer radius, Λ_t is the thermal-conductivity coefficient of the fiber material (silica), and h is the thermal-convection coefficient on the fiber–air boarder.

Finally, the overall change of refractive index Δn_Σ at the signal wavelength λ, when it is pumped at the wavelength λ_{pump}, is to be written as $\Delta n_\Sigma = \Delta n_{\text{res}} + \Delta n_{\text{therm}}$ that is a sum of the resonant [Eq. (3)] and thermal parts [Eq. (6)].

A comparison of the experimental measurements of the overall phase shift $\Delta\varphi_\Sigma$ and the corresponding change of refractive index Δn_Σ, exploiting the described above phase-modulated MFI technique, with the modeling, where Δn_Σ is determined with the use of Eqs. (2)–(7), is presented in Fig. 4 (the basic parameters taken at the modeling are listed in Table I). Here, the experimental and theoretical values of $\Delta\varphi_\Sigma$ and Δn_Σ are given for the different pump powers ($P_{\text{pump}}=35$ and 70 mW) in the spectral range of the signal wave, $\lambda=1500$–1580 nm. Note that the data in Fig. 4 for Δn_Σ (right axis) are determined from the data for $\Delta\varphi_\Sigma$ (left axis) with a correction given by the overlap factors Γ_i, addressing a match of the probe-beam Gaussian distribution in the fiber with: (1) the erbium-doped core-area ($\Gamma_1=0.44$, for determining the resonant part Δn_{res}) and (2) the region where the inhomogeneous temperature distribution $\Delta T(Q,r)$ [see

TABLE I. Parameters used in modeling.

	Parameter	Value
1	Refractive index thermal dispersion	$dn/dT=0.85\times10^{-5}$ K^{-1}
2	Total thermal gradient in silica jacketed fiber	$dS/dT\approx 2$ $dn/dT=1.7\times10^{-5}$ K^{-1}
3	Silica thermal conductivity	$A_t=0.014$ W/cm K
4	Thermal-convection coefficient	$h=0.5$–1.0 W/cm^2 K
5	Air surrounding teperature	$T_0=20$ °C
6	Radius of Gaussian signal-wave	$w_0=2.6\times10^{-4}$ cm
7	Multimode pump-beam cross section in fiber	$S_P\approx \pi r_0^2=6.34\times10^{-8}$ cm^2
8	Erbium^{3+} fluorescence lifetime	$\tau=1.0\times10^{-2}$ s
9	Small-signal absorption coefficient ($\lambda_{\text{pump}}=980$ nm)	$\alpha_0=0.0245$ cm^{-1}
10	Erbium^{3+} GSA cross section ($\lambda_{\text{pump}}=980$ nm)	$\sigma_{\text{GSA}}=1.2\times10^{-21}$ cm^2
11	Erbium^{3+} concentration in fiber	$N_0=2.1\times10^{19}$ cm^{-3}
12	Stokes-loss	$\xi=0.37$
13	ESA loss	$\varepsilon=0.43$

formula (7)] is established ($\Gamma_2=1$, for determining the non-resonant thermal part Δn_{therm}). The inset to Fig. 4 shows that the thermal contribution in the resultant refractive index change in the fiber linearly depends on the pump power.

One can see that the experimental data are perfectly fitted by the theory, which is a simple formulation of the nonlinear refraction problem for the case of a heavily doped erbium fiber in the conditions of optical pumping at the wavelength $\lambda_{\text{pump}}=980$ nm and an account of the KKR for the resonant refractive index change Δn_{res} and the ESA- and Stokes-induced heating, determining its thermal (nonresonant) contribution. Let us finally note that even in the case of rather low pump powers ($P\leq100$ mW) treated above, the thermal part in the overall refractive index change in the erbium fiber is a notable value; thus, one may suppose that for higher pump powers (W), it will have much more impact, especially on the fiber-based lasers and amplifiers where active fibers with a high concentration of erbium are used.

[1]E. Desurvire, J. Lightwave Technol. **8**, 1517 (1990).
[2]R. A. Betts, T. Tjugiarto, Y. L. Xue, and P. L. Chu, IEEE J. Quantum Electron. **27**, 908 (1991).
[3]J. W. Arkwright, P. Elango, G. R. Atkins, T. Whitbread, and M. J. F. Digonnet, J. Lightwave Technol. **16**, 798 (1998).
[4]D. C. Hutchings, M. Sheik-Bahae, D. J. Hagan, and E. W. VanStryland, Opt. Quantum Electron. **24**, 1 (1992).
[5]S. C. Fleming and T. J. Whitley, Electron. Lett. **27**, 1959 (1991).
[6]D. C. Brown and H. J. Hoffman, IEEE J. Quantum Electron. **37**, 207 (2001).
[7]P. A. Krug, M. G. Sceats, G. R. Atkins, S. C. Guy, and S. B. Poole, Opt. Lett. **16**, 1976 (1991).
[8]R. S. Quimby, W. J. Miniscalo, and B. Thompson, Proc. SPIE **1581**, 72 (1991).
[9]R. Rangel-Rojo and M. Mohebi, Opt. Commun. **137**, 98 (1997).
[10]A. V. Kir'yanov, N. N. Il'ichev, and Y. O. Barmenkov, Las. Phys. Lett. **1**, 194 (2004).
[11]H. Garcia, A. M. Johnson, F. A. Oguama, and S. Trivedi, Opt. Lett. **28**, 1796 (2003).
[12]E. Desurvire, "*Erbium-doped Fiber Amplifiers-Principles and Applications*" (Wiley, New York, 1994), pp. 295–302.
[13]N. Lagakos, J. A. Bucaro, and J. Jarzynski, Appl. Opt. **20**, 2305 (1981).
[14]L. C. Oliveira and S. C. Zilio, Appl. Phys. Lett. **65**, 2121 (1994).